Proc. Natl. Acad. Sci. USA
Vol. 90, pp. 7332–7335, August 1993
Biophysics

Three-dimensional waves of excitation during *Dictyostelium* morphogenesis

(chemotaxis/numerical simulations/self-organization/reaction–diffusion coupling)

OLIVER STEINBOCK*, FLORIAN SIEGERT†, STEFAN C. MÜLLER*, AND CORNELIS J. WEIJER†

*Max-Planck-Institut für molekulare Physiologie, Rheinlanddamm 201, D-4600 Dortmund 1, Federal Republic of Germany; and †Zoologisches Institut, Universität München, Luisenstrasse 14, D-8000 München 2, Federal Republic of Germany

Communicated by Howard C. Berg, April 1, 1993 (received for review January 4, 1993)

ABSTRACT **Cells in *Dictyostelium* slugs follow well-defined patterns of motion. We found that the chemotactic cell response is controlled by a scroll wave of messenger concentration in the highly excitable prestalk zone of the slug that decays in the less-excitable prespore region into planar wave fronts. This phenomenon is investigated by numerical solutions of partial differential equations that couple local nonlinear kinetics and diffusive transport of the chemotactic signal. In the interface of both regions a complex twisted scroll wave is formed that reduces the wave frequency in the prespore zone. The spatio-temporal dynamics of waves and filaments are followed over 33 periods of rotation. These results yield an explanation of collective self-organized cell motion in a multicellular organism.**

Spatio-temporal self-organization is a general phenomenon occurring in excitable media (1, 2). Propagating waves of excitation are observed in physical, chemical, and biological systems, as diverse as the CO oxidation on platinum (3), the Belousov–Zhabotinsky (BZ) reaction (4, 5), *Xenopus* oocytes (6), cardiac muscle (7), and the slime mold *Dictyostelium discoideum* (8, 9). In two dimensions, these systems show a variety of wave structures including concentric rings and spiral waves.

For wave patterns occurring during *Dictyostelium* aggregation, the underlying biochemical and cellular reactions are well investigated (10). The aggregation of single cells to form multicellular structures is directed by periodic signals of cAMP and chemotaxis. Cells in the aggregation center periodically produce the chemoattractant cAMP. The cAMP is secreted into the extracellular medium, where it diffuses away. Neighboring cells detect cAMP via cell surface receptors. The stimulated cells then produce huge amounts of cAMP, which they in turn secrete. This feedback process results in a wave-like propagation of the cAMP signal from cell to cell and from the aggregation center outward (10). Binding of cAMP to the receptor induces a phosphorylation of the receptor that leads to desensitization and the shut down of cAMP production. Extracellular phosphodiesterase degrades cAMP, which allows the system to recover. Immediately after stimulation the cells are refractory to further stimulation. This property ensures unidirectional outward propagation of the signal. Stimulated cells move chemotactically in the direction of increasing cAMP concentrations, thus producing periodic waves of inward-directed chemotactic movement. These waves are detected as optical density waves under dark-field illumination (9, 10).

Nonlinear differential equations coupling local reaction kinetics with diffusive transport can reproduce experimental observations on the BZ reaction and *Dictyostelium* aggregation qualitatively and quantitatively (11–14). Complex modes of wave propagation have been observed in three-dimensional reaction–diffusion systems (15)—e.g., scroll waves that emerge from a straight axis (filament). An untwisted scroll wave exhibits identical Archimedian spirals for each two-dimensional cut perpendicular to the filament. Such wave patterns have been studied in the BZ reaction (16, 17) and can undergo complicated changes in geometry as they travel along a gradient of excitability. For example, a scroll wave decomposes to a twisted scroll wave and then into planar waves when it propagates into a medium of lower excitability (18).

Recently, we have obtained (19) evidence that three-dimensional scroll waves organize the motion of cells in *Dictyostelium* slugs. The slug is a migratory stage during the developmental cycle of *Dictyostelium*, in which the behavior of 10^5 individual cells is coordinated to that of a single organism (Fig. 1). The direction of cell motion is controlled by propagating waves of cAMP concentration. Cell motion occurs in a direction opposite to the direction of wave propagation (10, 20). The anterior part of the slug (20% of all amebae) consists of prestalk cells, which ultimately build the stalk of the fruiting body. The remainder is formed by prespore cells that differentiate to spores in the fruiting body.

Model and Numerical Approach

Analysis of cell motion in slugs revealed that amebae in the prespore zone move straight forward in the direction of slug migration, whereas cells in the prestalk zone move perpendicular to the direction of slug migration, that is they rotate around the slug axis. This analysis suggested that the chemotactic signal spreads as a scroll wave in the front of the slug and converts into planar waves in the rear part. We proposed (19) that this complex mode of wave propagation was caused by a change in excitability along the long axis of the slug, based on the finding that during aggregation the cells that will become prestalk show high-frequency oscillations in optical density when isolated, whereas cells that will become prespore show slow oscillations (21).

To investigate whether an excitable system exhibits such behavior in three dimensions, we performed computer simulations. Martiel and Goldbeter (22) have developed a model that describes the process of receptor-mediated cAMP production and desensitization based on receptor phosphorylation. The three variables in this model take into account the extracellular cAMP concentration, the intracellular cAMP concentration, and the fraction of activated receptors. By assuming realistic values for rates of receptor phosphorylation and cAMP synthesis and degradation, this model could produce sustained cAMP oscillations. When coupled with diffusion, spiral wave propagation was observed. This model was reduced to a two-variable model that essentially shows

The publication costs of this article were defrayed in part by page charge payment. This article must therefore be hereby marked "*advertisement*" in accordance with 18 U.S.C. §1734 solely to indicate this fact.

Abbreviation: BZ, Belousov–Zhabotinsky.

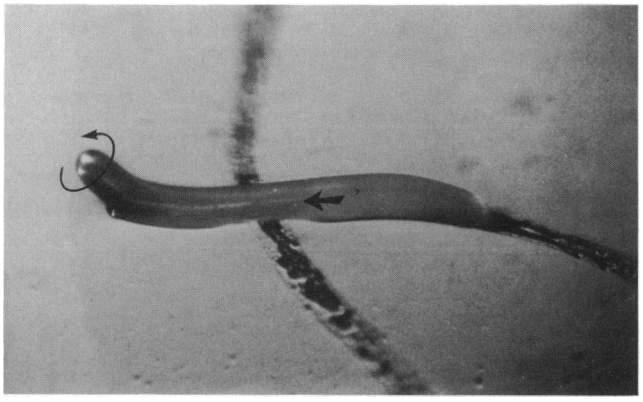

FIG. 1. *D. discoideum* slug. The tip (left side) rises up in the air. The prestalk zone (anterior 20%) is stained with the vital dye neutral red and is slightly darker in the photograph. The direction of cell motion is indicated by the arrows. In the prestalk zone, the cells rotate around the tip, whereas in the prespore zone (posterior 80%), the cells move forward in direction of the tip (18). The slug leaves a slime trail behind that is secreted by all cells. In the photograph, the slug crosses a slime trail left behind by another slug.

the same features such as oscillations and spiral wave propagation (22, 23).

Our main interest is to study wave propagation in an inhomogeneous excitable medium in three dimensions. This requires the numerical solution of sets of nonlinear partial differential equations. We have chosen the two-variable Barkley model (24) that produces the same features as the three-variable Martiel–Goldbeter model but is optimized for efficient numerical solution:

$$\frac{\partial u}{\partial t} = D_u \Delta u + \frac{1}{\varepsilon} u(1-u)\left(u - \frac{v+b}{a}\right)$$

and

$$\frac{\partial v}{\partial t} = u - v,$$

where diffusion coefficient $D_u = 1.0$ and parameters $a = 0.4$, $\varepsilon = 1/150$, and b specify the excitability of the system. The propagator u and the controller species v are functions of time and the three spatial coordinates. The variable u obeys nonlinear reaction kinetics and qualitatively models the extracellular cAMP concentration, and v represents the fraction of the cAMP receptors in the active state. The shape of the *Dictyostelium* slug is approximated by a cylinder (length, 100 grid points; diameter of cross section, 34 grid points). The total number of grid points (90,800) is of the same magnitude as the number of amebae in a typical slug. The cylinder is embedded in a rectangular box, surrounded by grid points obeying unexcitable kinetics ($b = 0.3$). Consequently, a flux of u through the cylindric boundary takes place, simulating loss to the slime sheath covering the slug. The difference in excitability between the prestalk and prespore region is modeled by a step function of parameter b along the symmetry axis of the cylinder ($b_{pst} = 0.01$ and $b_{psp} = 0.023$).

The diameter L of the circular cross section and the time step Δt are chosen to be $L = 21.25$ and $\Delta t = 0.041$. The Laplacian term is estimated from the six closest neighboring points. All calculations were performed on a Sun-IPX workstation and visualized by Sunvision software.

Results

The initial condition is an untwisted scroll wave along the long axis of the slug having constant excitability ($b_{pst} = b_{psp} = 0.01$) that stably rotates in the homogeneous system. After some time ($t = 880$ iterations), a change in excitability along the slug's long axis, as described above, is introduced. The scroll wave undergoes a complex transformation into a new pattern, as shown in the image sequence in Fig. 2. While the wave rotation in the region of high excitability (prestalk region) remains stable during the entire calculation, the scroll wave in the region of low excitability (prespore region) increases its wavelength and rotation period. Subsequently, the whole structure becomes twisted in middle segments of the cylinder (Fig. 2*A*). The process of twisting and the higher frequency in the prestalk region cause a dramatic change of

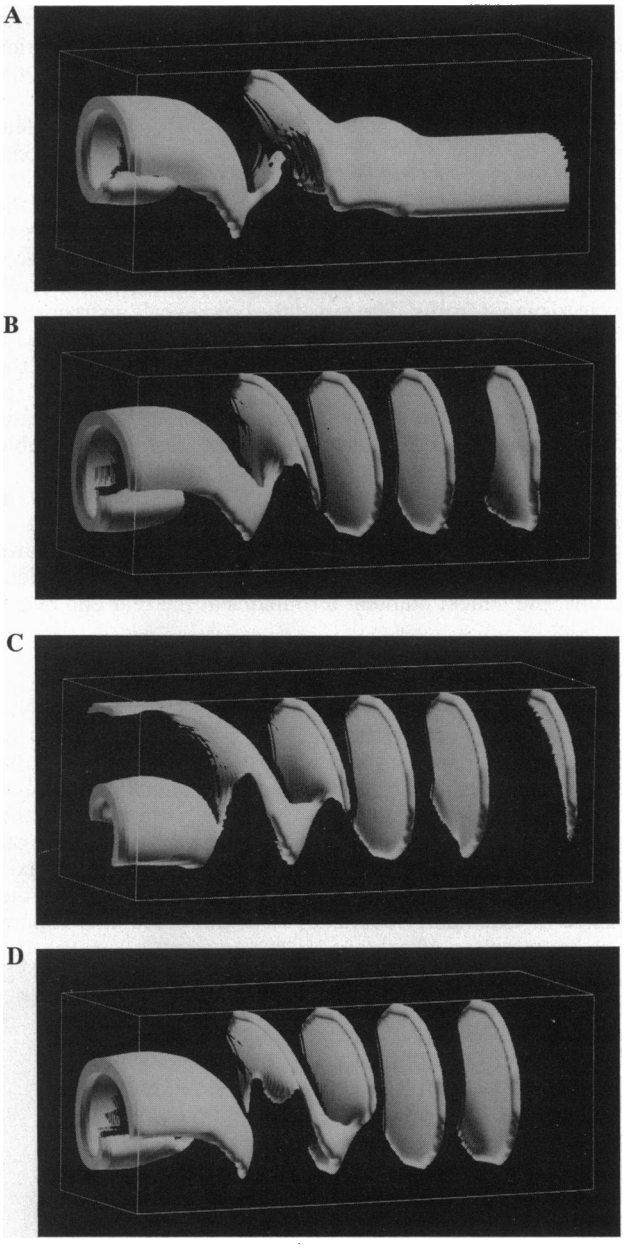

FIG. 2. Three-dimensional representation of the variable v ($v < 0.27$ transparent). The cylindrical excitable medium is separated in a high-excitable (left 20%, prestalk zone) region and a low-excitable (right 80%, prespore zone) region. The step of excitability destroys the initial scroll wave (*A*) and transforms it into planar waves in the right part (*B–D*). The depicted combination of wave structures explains the coordination of chemotactic cell motion in *Dictyostelium* slugs (see Fig. 1). Relative times of the pictures: t_a, 2600 iterations; t_b, 7800; t_c, 8000; t_d, 8200. The excitability step is initiated after 880 iterations.

the pattern in the less-excitable prespore zone: Planar wave fronts appear that are oriented perpendicular to the long axis of the cylinder (Fig. 2 *B–D*). Detailed analyses show that the shape of these wave fronts is slightly convex, thus focusing cell motion and stabilizing the slug geometry. This spatial arrangement is then stable over more than 30 periods of scroll wave rotation. The interface between the region of scroll wave rotation and planar wave propagation displays more complex dynamics and alternating phases of weak and strong twisting.

Fig. 3 showing the filament of wave rotation helps to elucidate the dynamics of this region. While the filament in the prestalk zone is generally oriented along the long axis of the slug, it becomes helical at the interface and bends away from the axis before ending at the cylinder boundary. Movies of the filament evolution reveal irregular changes in location and shape, but most of the time it stays attached to the boundary.

The space–time portrait in Fig. 4 describes dynamic features of the simulation. It consists of 324 two-dimensional spatial cuts (40,000 grid points) of the cylinder. The time between each spatial cut is 50 iterations. The left side of the space–time box (the prestalk zone) shows unperturbed wave propagation, and the right side shows the less-excitable prespore region and illustrates the decay of the initial scroll wave to planar fronts. The top of the box reveals an important consequence of the alternating wave form in the interface. Some of the emitted waves disappear at the right side of the interface or fuse with following ones. This mechanism reduces the number of waves in the prespore region and leads to frequencies that can be supported by this less-excitable medium.

The described behavior occurs in a range of values of b in the prespore region (e.g., $b_{psp} = 0.0245, 0.026$). For values of b_{psp} smaller than 0.021, the whole prespore region shows twisted scroll waves with large wavelengths. In these calculations, the helical filament terminates at the rear end of the cylinder.

Conclusions

Our calculations demonstrate that the observed pattern of chemotactic cell motion in *Dictyostelium* slugs (19) can be readily explained by scroll waves of a chemotactic signal in the prestalk zone that decay into planar wave fronts in the prespore zone. This change in the pattern of wave propagation is caused by a change in excitability along the long axis of the slug. The data are well fitted by the assumption that the change in excitability coincides with the prestalk–prespore boundary. The simulations have, furthermore, shown that the filament of the scroll wave in the prestalk zone is a stable structure, a region of steady and low concentration of the excitation variable, conditions that most likely direct stalk formation by controlling expression of stalk-specific genes (19).

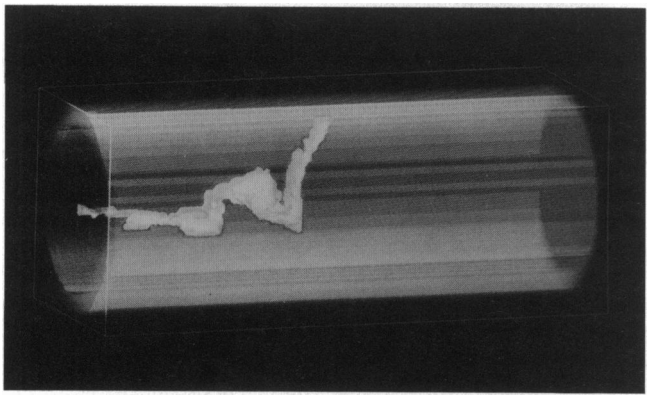

FIG. 3. Filament of wave rotation and boundary between the cylindrical excitable region and the unexcitable surroundings. The filament describes the set of spatial points having a low maximum value of u and v during one rotation of the scroll wave (420 iterations). Calculations are after 26 periods of scroll wave rotation.

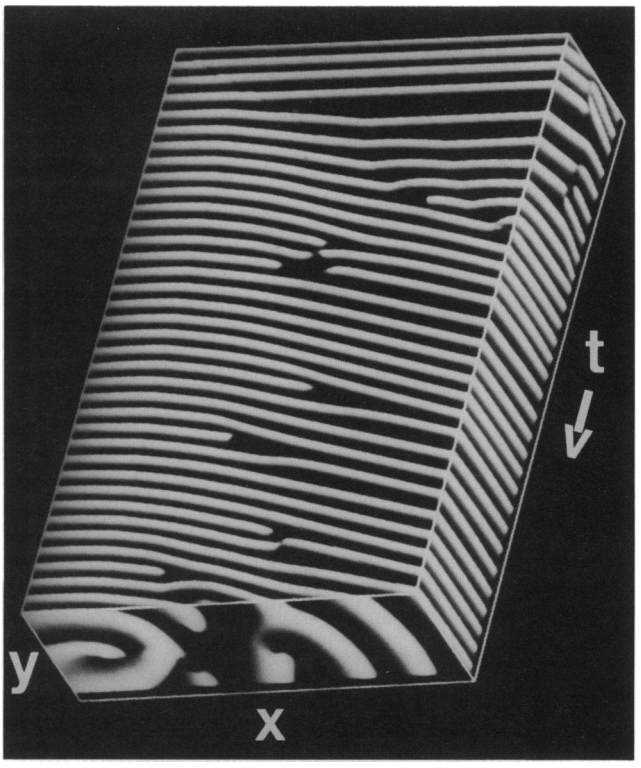

FIG. 4. Space–time portrait (x, y, and t) constructed from two-dimensional spatial cuts along the symmetry axis of the cylinder. The front side of the box shows the last (t = 16,200 iterations) spatial cut. The high-excitable prestalk zone is located on its left side, depicting a cut of the scroll wave that decays to perpendicular wave fronts. The top view illustrates the temporal transformation of scroll wave fronts (horizontal stripes) into waves propagating into the right prespore zone (tilted stripes).

These simulations explain the coordination of collective motion in a multicellular organism. They show that waves of excitation play a crucial role not only during aggregation but also during later three-dimensional morphogenesis in *Dictyostelium*. Our results also provide a simple explanation for complex modes of wave propagation in inhomogeneous excitable systems such as specific three-dimensional BZ media (18) or cardiac muscle (7).

1. Swinney, H. L. & Krinsky, V. I., eds. (1991) *Waves and Patterns in Chemical and Biological Media, Physica D* (North-Holland, Amsterdam), Vol. 49.
2. Markus, M., Müller, S. C. & Nicolis, G., eds. (1988) *From Chemical to Biological Organization* (Springer, Berlin).
3. Jakubith, S., Rotermund, H. H., Engel, W., von Oertzen, A. & Ertl, G. (1990) *Phys. Rev. Lett.* **65**, 3013–3016.
4. Zaikin, A. N. & Zhabotinsky, A. M. (1970) *Nature (London)* **225**, 535–537.
5. Field, R. J. & Burger, M., eds. (1985) *Oscillations and Travelling Waves in Chemical Systems* (Wiley, New York).
6. Lechleiter, J., Girard, S., Peralta, E. & Clapham, D. (1991) *Science* **252**, 123–126.
7. Davidenko, J. M., Pertsov, A. V., Salomonsz, R., Baxter, W. & Jalife, J. (1992) *Nature (London)* **355**, 349–351.
8. Tomchik, K. J. & Devreotes, P. N. (1981) *Science* **212**, 443–446.
9. Siegert, F. & Weijer, C. J. (1989) *J. Cell Sci.* **93**, 325–335.
10. Devreotes, P. N. (1989) *Science* **245**, 1054–1058.

11. Keener, J. P. & Tyson, J. J. (1986) *Physica D* **21,** 307–324.
12. Tyson, J. J. & Murray, J. D. (1989) *Development* **106,** 421–426.
13. Foerster, P., Müller, S. C. & Hess, B. (1990) *Development* **109,** 11–16.
14. Foerster, P., Müller, S. C. & Hess, B. (1988) *Science* **241,** 685–687.
15. Winfree, A. T. (1990) *SIAM* **32,** 1–53.
16. Welsh, B. J., Gamatam, J. & Burgess, A. E. (1983) *Nature (London)* **304,** 611–614.
17. Tzalmona, A., Armstrong, R. L., Menzinger, M., Cross, A. & Lemaire, C. (1990) *Chem. Phys. Lett.* **174,** 199–202.
18. Yamaguchi, T. & Müller, S. C. (1991) *Physica D* **49,** 40–46.
19. Siegert, F. & Weijer, C. J. (1992) *Proc. Natl. Acad. Sci. USA* **89,** 6433–6437.
20. Steinbock, O., Hashimoto, H. & Müller, S. C. (1991) *Physica D* **49,** 233–239.
21. Weijer, C. J., MacDonald, S. A. & Durston, A. J. (1984) *Differentiation* **28,** 13–23.
22. Martiel, J.-L. & Goldbeter, A. (1987) *Biophys. J.* **52,** 807–828.
23. Tyson, J. J., Alexander, K. A., Manoranjan, V. S. & Murray, J. D. (1989) *Physica D* **34,** 193–207.
24. Barkley, D. (1991) *Physica D* **49,** 61–70.